Passive characterization of hydrofracture properties using signals from the hydraulic pumps

DP1.3

James W. Rector, III and Qicheng Dong, University of California, Berkeley*

Summary

In this study we utilize conical shear wave arrivals recorded in geophone observation wells to characterize a hydrofracture performed in the South Belridge Diatomite oil field (Vinegar, et al, 1991). The conical wave arrivals are initially created by the hydraulic pumps on the surface, which send tube waves down the treatment borehole. Since the tube wave velocity in the Diatomite is greater than the shear formation velocity (the shear velocity in the diatomite is about 2,200 ft/s) conical shear waves are radiated into the formation by the tube waves traveling down the treatment borehole. We use the decrease in amplitude of the tube wave as it passes through the fracture zone to image changes in hydraulic conductivity of the fracture. By combining this information with estimates of the fracture height (from Ilderton, 1994) we obtain estimates of fracture width changes over time using the model of Tang and Cheng (1993). We find an excellent qualitative agreement between tube wave attenuation and pump pressure over time. Fracture widths estimated from the Tang and Cheng model appear to be consistent with the volume of injected fluid and the known length of the hydrofracture (Ilderton, et al 1993). Provided a monitor well can be instrumented, this technique holds potential for obtaining a relatively inexpensive real-time characterization of hydrofracs.

Introduction

Hydrofracturing is a common technique used to enhance the effective wellbore radius from which hydrocarbons are pumped in low- to moderate permeability formations. A properly executed hydrofrac results in a 'path' connected to the well, that has a higher permeability than the surrounding formation (frequently five to six orders of magnitude, Economides, et al, 1993). The geometry of the hydrofracture is critical to the amount of enhanced productivity that the well experiences. For example, in lower permeability reservoirs that are stimulated by hydrofracing, the fracture length is of primary importance while the hydraulic conductivity of the fracture is of secondary importance. In higher permeability reservoirs, the fracture permeability is the most important factor controlling enhanced production. There is a strong motivation to understand fracture geometry and the mechanisms that control fracture geometry. With a knowledge of fracture geometry after the fact, proper locations for infill wells can be determined. With a knowledge of fracture properties in real time, modifications can, in principle, be made to injection rates, time periods, and slurry concentrations to optimize fracture geometry and fracture permeability.

Hydraulic fracture shapes are quite variable and depend on the in-situ mechanical properties in the vicinity of the treated well and the volume, type and rate of the injected fluids. Fracture characterization is normally done using injection rates and wellhead pressure measurements. For example, in the PKN model (Economides, et al, 1993) the fracture width at any time during the fracture, $w(t)$, is proportional to $x(t)^{1/4}q(t)^{1/4}$ where $x(t)$ is the fracture half-length and $q(t)$ is the injection rate. From plots of the net downhole pressure versus time (typically inferred from the surface wellhead pressure), reservoir engineers infer the morphology of the propagating fracture. When the slope is positive, a normally extending, vertically-contained fracture is inferred. When the slope is negative, fracture height grows faster than fracture length (a generally undesired characteristic). These model-based fracture characterization techniques require accurate knowledge of the formation mechanical properties and the in-situ stress magnitudes. In the real world, vertical and lateral heterogeneities and local borehole conditions require much more complex models than are currently available. Consequently, reservoir engineers are quite interested in more direct methods of fracture imaging using geophysics.

An extensive experiment was carried out by Shell Oil Co. in the South Belridge Diatomite oil field near Bakersfield, Ca. in 1990 to image fracture geometry using microseismic events recorded by a three-borehole array of cemented downhole geophones and shear wave shadowing using airgun sources in a nearby borehole (Vinegar, et al, 1991). Analysis of the microseismic events produced during an injection fracture (Ilderton, 1994) demonstrated that the fracture azimuth was N21E or roughly perpendicular to the minimum in-situ stress direction and that most of the microseismic event activity occurred in the more permeable zones (roughly 100 ft within a 400 ft perforation interval). Significant asymmetry was observed in the upper injection fracture (IN2U), with most of the microseismic events occurring to the NE of the injection well, and very little to the SW. The microseismic event locations were found to be consistent with temperature observations during later steam flooding of the hydrofractured reservoir, indicating that microseismic events accurately predicted the fracture direction and the vertical and horizontal extent of the fractured interval.

Description of the Hydrofracture Experiment

We performed the tube wave attenuation analysis on a hydrofracture performed in the IN2U well during 1990. Figure 1 shows a map view and Figure 2 shows a cross-sectional view of the recording geometry, The treatment borehole, IN2U, was drilled to a depth of 1620 ft, and was perforated between 1120 and 1450 ft. The observation wells, MO-1, MO-2, and MO-3 were located zft, y ft, and x ft from the injection well. The borehole used for the airgun source, LO-13, was located j ft from IN2U.

The hydrofracture was performed in stages. The minifrac, performed on day 1 of the hydrofracture consisted of 5 separate stages, each lasting about 10 minutes. The average pump pressure was 200 psi, and the injection rate varied between 1 and 26 bpm during pumping. The total volume of injected fluids was 940 bbl in the minifrac and 2727 bbl in the main fracture. After the minifrac, the well was shut in for 3 days to allow KCl to percolate into the microfractures, and then on day 5 the main fracture was performed. The average pump pressure for the main fracture was 300 psi and the injection rate varied from 15 to 26 bpm, the total volume of slurry was 1510 bbl.. The main fracture lasted about 4 hours.

Generation and Propagation of Conical Shear Waves

Analysis of the airgun data and the microseismic events by Ilderton (1994) showed that strong shear-conical waves were produced by the

airgun source and that primarily shear wave arrivals from microseismic events were recorded by the observation geophones. An example of an airgun-generated conical wave is shown in Figure 3. Note the linear moveout of the arrival at an apparent velocity of 4,300 ft/s. A hypothetical wavefront and raypath for the airgun-generated conical wave is shown in Figure 2. The takeoff angle, β, is related to the contrast between the shear velocity of the formation and the fluid velocity. We believed that similar conical waves should also be produced by dynamic pressure variations in the treatment well (IN2U). These conical wave are also depicted in Figure 2.

The far-field conical wave arrival undergoes two types of attenuation. The first type of attenuation is geometric spreading, which for a conical wavefront is proportional to $r^{-1/2}$, where r is the radial distance from the borehole. The other type of attenuation is related to attenuation of the tube wave traveling up or down the borehole. The tube wave is essentially the 'core' of the conical wave. It is well known that tube waves undergo transmission losses at borehole diameter changes, formation property changes, and most importantly for our purposes, fracture zones and changes in formation permeability (Tang and Cheng, 1993).

Using Conical Wave Attenuation to Obtain Tube Wave Attenuation in the Fracture Zone

Our approach to characterizing the hydrofracture was to use the change in tube wave attenuation over the fracture zone over the time history of the hydrofrac. The tube wave attenuation is reflected by changes in the received conical wave arrival amplitude. We assume that the treatment-well conical wave amplitude at a shallow geophone depth (see figure 2) above the fracture zone only varies with pump pressure. If we ignore frequency dependent effects we can approximate the conical wave arrival amplitude, $A_u(t)$ by:

$$A_u(t) = S(t)E_u, \qquad (1)$$

where $S(t)$ is the source amplitude (related to the pump pressure) and E_u is the attenuation due to propagation through the earth between the treatment well and the upper geophone. The conical wave arrival amplitude at some lower geophone position, $A_l(t)$, will be given by

$$A_l(t) = S(t)E_lB(t), \qquad (2)$$

where $S(t)$ is as before, E_l is the attenuation through the earth between the treatment well and the lower geophone, and $B(t)$ is the loss in amplitude of the tube wave in the treatment well as it travels through the fracture zone. We will assume that E_u and E_l are constant with time, which is probably valid if we use geophone wells nearly perpendicular to the fracture azimuth (the formation properties in the fractured interval only change as a function of frac history along the fracture azimuth.) By computing the amplitude ratio of the upper and lower geophones we obtain:

$$A_u(t)/A_l(t) = E_u/E_lB(t), \qquad (3)$$

and the pump pressure is removed from the expression. If we further only examine changes in amplitude over fracture history (time) we eliminate E_u/E_l and isolate $B(t)$.

Initial analysis of the hydrofracture data indicated that the sought-after conical wave arrivals from the treatment well pumps were easy to detect in the raw data after lowpass filtering (10 to 120 Hz) (figure 4). In fact the frequency spectra of this data showed resonance peaks that we believe are related to the pump frequency. These strong conical wave arrivals were apparent whenever pump pressure (source amplitude) was high. The most coherent conical wave arrivals were observed at the MO-2 well, which is closest to the treatment well. The weakest conical wave arrivals were observed at the MO-1 well which is nearly in line with the fracture azimuth.

Time-Dependent Changes in Conical Wave Amplitudes during the Hydrofrac

Figure 5 is a plot of the amplitude (computed over a 16s window) of two geophones in the MO-2 well during the five stages of the minifrac and the seven stages of the main frac. The top geophone is located at a depth of 1043 ft, while the bottom geophone is located at a depth of 1546 ft. Ilderton (1994) showed that most of the microseismic events during the main fracture occurred between 1250 and 1350 ft. The pump pressure is given at the top of the figure. Figure 5 shows a classic pressure distribution from a hydrofrac, where the pressure increases rapidly at first followed by a rapid decline at breakdown, and a more gradual drop in pressure thereafter.

Note the correspondence between time dependent amplitude changes on both geophones and pump pressure, suggesting that pump pressure changes are the predominant cause of time-dependent amplitude changes. The geophone amplitudes are identical when the pump pressure is low, indicating that the earth transmission properties for the conical wave are roughly the same for each geophone ($E_u = E_l$).

Figure 6 shows the amplitude ratio between the two geophones plotted as a function of minifrac history. As expected from Figure 5, the amplitude ratio between the top and the bottom geophone increases dramatically when the pump pressure is high, indicating an increase in the tube wave attenuation due to the opening of fractures (increase of permeability) in the fracture zone. In fact, we can see that for the first three pump stages, the ratio increases over time during the periods of high pump pressure, suggesting that the fracture zone permeability is increasing. At each stage of the minifrac the ratio is higher that the previous stage which means that the fracture zone permeability is being increased during each of the three stages. The anomaly is the fourth/fifth stage where it does not appear from the pressure history that breakdown ever occurred . This is confirmed by the amplitude ratio, which never grew to large levels as in the three previous stages where breakdown did occur.

Figure 7 shows the amplitude ratios in the main frac. There are several interesting things to note about Figure 7. First, the baseline amplitude ratio is about 2.5, whereas in the minifrac the baseline amplitude is about 1.0. We believe that the minifracs caused very small (< 20 Angstroms) fractures near the wellbore that were not immediately filled by fluid and therefore did not immediately attenuate the tube waves traveling down the borehole. After three days these smaller fractures were opened through the process of adsorption. Once opened these smaller fractures increased the permeability of the fracture zone and the baseline amplitude ratio increased.

Another interesting phenomena from Figure 7 is the gradual increase in ratio during the main fracture, indicating that the fracture permeability continued to increase during the entire period of high pump pressure. It is generally assumed that fracture permeability is related to fracture width which increases as the fracture extends in height or length. Thus we could interpret the continued increase in amplitude ratio over the entire period of high pressure as an indication that the fracture is continuing to extend. Provided that we could constrain the fracture height growth (by comparing conical wave arrivals from tube waves bracketing the fracture zone) we could use

the changes in amplitude ratio to inform the reservoir engineer when the fracture has stopped growing. From the amplitude ratios in Figure 7 it appears that by using a lower injection rate the fracture could have been extended a greater distance prior to breakdown.

To estimate fracture aperture, we input the ratios of Figure 6 and 7 into the theoretical relationships derived by Tang and Cheng (1989, 1993). We used the relationship between fracture aperture and tmamission coefficient developed for a single fracture in Tang and Cheng (1989) to relate changes in fracture aperture to changes in transmission coefficient across the fracture zone. However to obtain estimates of the actual fracture aperture we assumed a fracture zone rather than a single fracture (Hornby, et al, 1992). Figure 8 shows the estimates of fracture aperture as a function of time. The average fracture aperture in the main fracture is about 2.3 mm, which is consistent with fracture models for the Diatomite (Patzek, 1995). Using the estimate fracture aperture, we estimated the total volume of the fracture zone (assuming fracture height, width and length based on the microseismic data). The total volume estimated is somewhat less than the total volume of injected fluids, which means that some percentage of fluids is leaking into the formation. Interestingly, the measured volume of the fracture could be compared with the volume of injected fluids to estimate a leakoff coefficient. The leakoff coefficient is critical to estimating the economic viability of a hydraulic fracture (Economides, et al, 1993).

Conclusions

We have shown that shear conical waves produced by hydraulic pumps during the hydaulic fracturing of a well can be used to estimate the fracture zone aperture though the use of tube wave transmission losses. The fracture apertures estimated by computing the amplitude ratio of shear conical waves recorded above the fracture zone to shear conical waves below the fracture zone are consistent with fracture models for the Diatomite.

Acknowledgments

This work was supported by SubContract #AI-7683 from Sandia National Laboratories. Norm Warpinski of Sandia and Steve Wolhart and Iraj Salehi of GRI were instrumental in initiating this project. The data was provided to Professor Tad Patzek of UC-Berkeley by Shell Oil Company.

References

Economides, M. J., Hill, A. D., and Ehlig-Economides, C., 1994, Petroleum production systems, Prentice-Hall.

Tang, X. M., and Cheng, C. H., Borehole stonely wave propagation across permeable structures, Geophys. Pros., 41, 165-187.

Tang, X. M., and Cheng, C. H., 1989, A dynamic model for fluid flow in open borehole fractures, JGR, 94, 7567-7576.

Hornby, B. E., Luthi, S.M., and Plumb, R. A., 1992, Comparison of fracture apertures computed from electrical borehole scans and reflected Stonely Waves.

Patzek, T., 1995, Personal communication.

Vinegar, H.J., Wills, P.B., DeMartini, D. C., Shlapobersky, J, 1991, Active and Passive Seismic Imaging of a Hydraulic Fracture in Diatomite, SPE 22756, Proceedings of SPE Ann. Tech. Conf. and Exhib., Dallas, Tx.

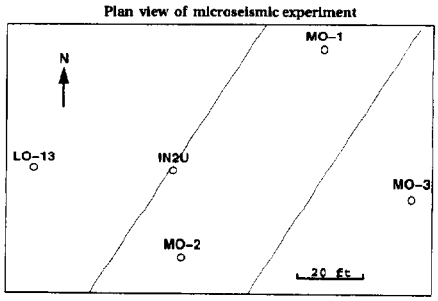

Figure 1: Map View of the injector (IN2U) hydrofracture imaging experiment in the South Belridge Diatomite. LO13 is the airgun well.

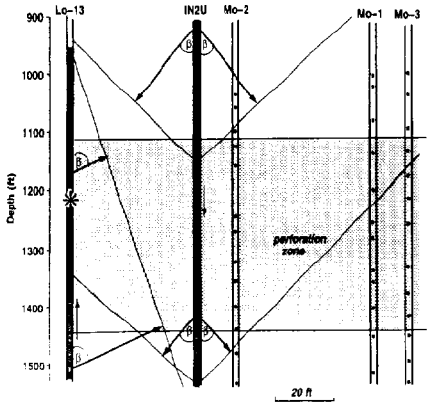

Figure 2: Cross-sectional view of the hydrofracture imaging experiment. Conical shear waves, with ray takeoff angle β are depicted as emanating from tube waves in both the airgun and the treatment well (IN2U). The downgoing tube waves in IN2U are produced by the hydraulic pumps at the surface.

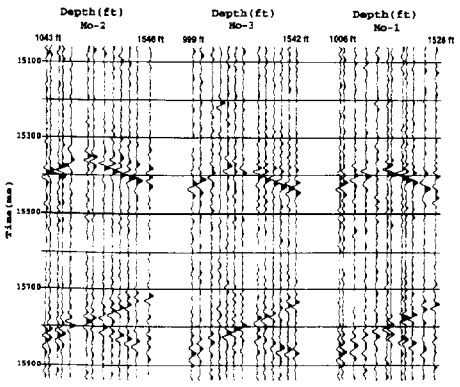

Figure 3: Example of conical shear waves recorded in the geophone observation wells and produced by the airgun.

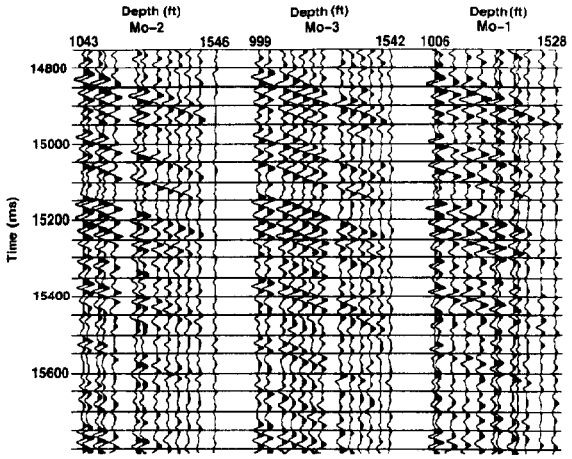

Figure 4: Example of periodic conical shear waves produced by tube waves in IN2U.

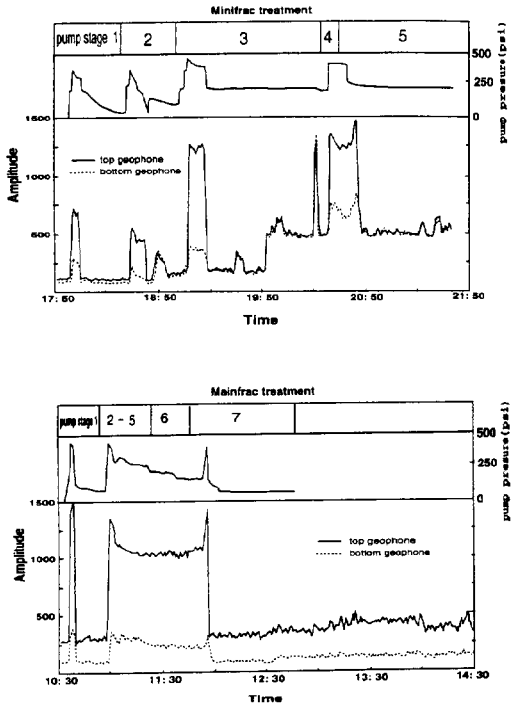

Figure 5: Amplitude as a function of time for two geophones in MO-2. (a) minifrac stages (b) main frac. The top geophone is located at 1043 ft, above the fractured zone, while the bottom geophone is located at 1540 ft, below the fracture zone. Note the correspondence between the amplitude and the wellhead pressure.

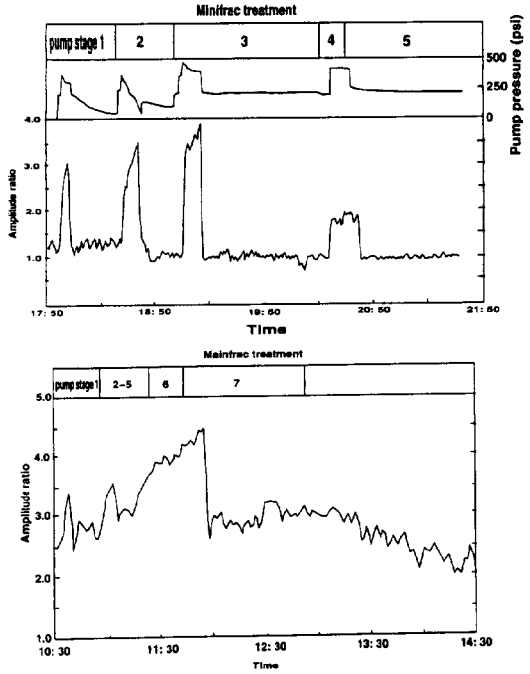

Figure 6: Amplitude ratio between top and bottom geophones in the minifrac. Note that the ratio increases when the pressure drops and the fracture opens.

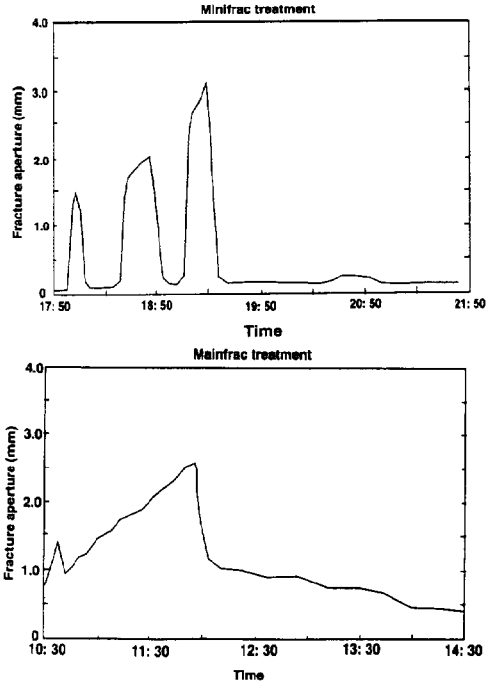

Figure 7: Amplitude of the top and bottom geophones in the main frac. Note that the ratio increases when the pressure drops and the fracture opens. Also note that the ratio continues to increase for the entire period of high pressure implying that the fracture is continuing to grow up to breakdown.